High Voltage

Research Article

IET Journals
The Institution of Engineering and Technology

Transformer components impact on compatibility of measured PDs: comparison of IEC60270 and RF methods

ISSN 2397-7264
Received on 21st July 2018
Revised 26th November 2018
Accepted on 13th December 2018
E-First on 4th February 2019
doi: 10.1049/hve.2018.5067
www.ietdl.org

Keyvan Firuzi[1], Mehdi Vakilian[1] ✉, B. Toan Phung[2], Trevor Blackburn[2]

[1]*Electrical Engineering Department and Centre of Excellence in Power System Management and Control, Sharif University of Technology, Tehran, Iran*

[2]*School of Electrical Engineering & Telecommunications, University of New South Wales, Sydney, Australia*

✉ *E-mail: vakilian@sharif.ir*

Abstract: Power transformer partial discharge signal measurement using Radio Frequency method has advantages over IEC 60270 'apparent charge' measurement method for online monitoring due to greater immunity against external interference. However, the lack of a well-defined calibration relationship between the two methods is main disadvantage of RF method. Simultaneous measurements, using these two methods, carried out on various transformer PD source models, in laboratory, to investigate main parameters that affect the relationship of results of these two methods. In this paper, factors that influence this relationship are classified into three groups: (i) type of PD sources, (ii) transformer windings as PD signal transmitter, and (iii) the inner structure of the transformer. Firstly, the relationship between these two methods has been investigated for some simple types of PD sources. Subsequently, by adding the winding structure model to the void, which is the PD source, its impact on each measurement method and the relationship between them have been studied. The impact of inner structure on the relation between the two methods is compensated through a formula which is proposed as a means for calibration of the RF partial discharge measurement setup. However to compensate for internal insulating system effects more research is required.

1 Introduction

Condition monitoring of power system equipment (especially insulation systems of very expensive equipment) improves plant economy, increases its reliability, availability and useful service life. Online condition monitoring of the power system equipment results in early detection of defects which helps the operator to minimise the unpredictable interruption of service, and to improve the service reliability. Additionally, use of available remedial measures will increase the lifetime expectancy of the equipment [1].

Partial discharge (PD) measurement is a popular condition monitoring technique that can reliably detect incipient faults and prevent a power transformer from having a major unexpected damage. Owing to these benefits a number of PD detection schemes have been developed over the past years. Two major PD test techniques of different types used for this purpose are (i) PD testing according to the international IEC60270 standard and (ii) the radio-frequency (RF) PD test method [2]. The measurement frequency bandwidth for RF systems is in both the very-high-frequency (HF) (30–300 MHz) and the ultra-HF (UHF) (300–3000 MHz) ranges.

The IEC60270 method has many advantages including active source separation [3], possible identification of active sources [4] and even online monitoring. However, the existence of different types of electrical noises makes it difficult to apply in all cases [5]. The advantage of the IEC60270 method is that it can be calibrated, so that the severity (magnitude) of the detected PD signals can be determined [6].

The main concept of the RF PD measuring technique is that PD current pulses have a rise time in the order of nanoseconds: for example, the rise time of PD signals from a protrusion PD source in oil is 0.9 ns [7]. Such fast pulses generate electromagnetic (EM) radiation within the range of the RF spectrum [8].

The UHF method has a better immunity to the externally sourced electrical noise due to the better shielding effect of a transformer tank at the higher frequencies.

The IEC60270 method attempts to quantify displaced PD charge (the integral of PD current) regardless of charge motion. The RF method responds to the dynamics of PD charge motion (the time derivative of PD current). Obviously, the two quantities are not necessarily proportional [9]. Therefore, the most important factor in the relationship between the IEC60270 and RF methods is the PD current pulse shape, which depends on the type of PD source [9, 10]. If there is a relationship between these two methods, the question to be asked is how the other factors such as the configuration of transformer internal components can change this relationship.

The complex interior structure of a transformer offers many obstacles to the propagation of the EM waves from PDs. Therefore, the study of the EM phenomena inside a transformer becomes more complex. Owing to this complex structure, the relationship between the signals detected using the RF and International Electric Commission (IEC) methods is influenced by factors such as the transformer winding, the PD source distance from PD sensor probe, the insulation system structure and the transformer tank [11].

The purpose of the research reported here is to quantify the RF/IEC relationship under controlled laboratory conditions using well-defined test samples. In this paper, the effect of each parameter on the recorded RF signals is investigated. For this purpose, the factors that can have impact on this relationship are divided into three categories:

- *PD source type*: This determines the existence and type of the quantifiable relationship between these two methods.
- *Transformer winding*: This acts as a signal transmitter for the IEC60270 method and a wave radiator for the RF method. Therefore, it can have some effect on both methods.
- *Inner transformer structure*: The transformer internal structure such as the insulating system affects both methods. The tank structure and the distance between PD source and the RF probe only affect the RF method.

The rest of this paper is organised as follows: In Section 2, the experimental setup used for simultaneous measurement of IEC60270 and RF method is introduced. In Section 3, the relationship between the two methods has been investigated for

This is an open access article published by the IET and CEPRI under the Creative Commons Attribution-NonCommercial-NoDerivs License (http://creativecommons.org/licenses/by-nc-nd/3.0/)

various PD sources. In Section 4, the effect of the transformer winding on both methods and the ratio between them and also the current pulse shape and received RF wave are investigated. In Section 5, the effects of the inner structure of transformer including the insulation system (using a sample small transformer model), the transformer tank characteristics and the distance between PD source and the RF probe have been studied. Section 6 concludes and gives the summary.

2 IEC60270 and RF methods

The experimental setup used in this work is shown in Fig. 1. The laboratory tests for the PD measurements are carried out inside a closed metallic tank (a Faraday cage) with dimensions of 6 m × 6 m × 4 m. A 300 pF capacitor is used as a coupling capacitor for the IEC test method. PD current pulses are captured using a measuring impedance. The corresponding RF waves emitted by the PDs are measured by the RF antenna.

A conical monopole antenna with a length of 10 cm and a diameter of 4 cm is used as an RF probe for receiving the PD EM waves. The benefits of using the conical shape are a wider bandwidth, a higher gain and a higher voltage standing wave ratio [12]. As a monopole antenna, the conical design is nearly omnidirectional and also can be installed through oil drain valves [13].

The PD current pulses and RF waves were recorded simultaneously using a 1 GHz bandwidth digital oscilloscope with maximum sampling rate of 5 G samples/s. Each pulse was captured over a duration of 12 µs and charge amplitude (Q), using a bandpass filter with centre frequency of 300 kHz and bandwidth 400 kHz, and RF signal voltage peak (V_p), are measured by means of the oscilloscope. In the RF signal measurement, no pre-amplifier is used.

3 PD signal source

To investigate the effect of the PD source on the $Q - V_p$ relationship, simultaneous measurement of the PD current pulse and the RF signal were carried out for the six PD sources, using the setup in Fig. 1.

Six artificial PD models, as shown in Fig. 2, are used in this paper. Since 'corona' and 'discharge in oil' and also 'surface discharge in air' and 'surface discharge in oil' models employ the same electrode configuration (first one located in air and the second one located in oil), one figure represents both. These six, can be represented by four different electrode configurations as shown in Fig. 2.

The PD source models (except the corona and surface discharge in air) were placed inside the test cells which are filled with transformer oil. The corona model is constructed by a needle-plane electrode (Fig. 2*a*). The internal discharge PD model is simulated by a sandwich structure of transformer paper including a cylindrical void of 4 mm diameter in its middle layer (Fig. 2*b*). Surface discharge PD is simulated using a sphere-plane electrode geometry with one layer of transformer paper in between (Fig. 2*c*). A floating particle PD model is developed by a sphere-plane electrode geometry (Fig. 2*d*). The gap distance between the two electrodes is adjusted to 15 mm. Free metal particles simulated using the cylindrical steel particle with a diameter of 0.5 mm and the maximum length of 3 mm. Spherical electrode made of aluminium, with 5 cm diameter and the plane electrode made of copper, with 10 cm diameter.

The PD measurements are performed with application of an AC voltage. The voltage is increased in small steps to reach the PD inception voltage for each model. The conical antenna is located at a 0.5 m distance from the PD source. The measured value of V_p is presented in mV and the IEC charge Q is presented in pC. The results of these measurements using the six PD model sources are shown in Fig. 3.

Except for the void discharge, which has a quadratic relationship, a linear relationship exists for the other five sources. The relationship of the two forms of PD results can be expressed including PD pulse polarity (positive or negative) through (1). The second equation is the relationship for the void model

$$\begin{aligned} V_p &= a_p Q(\text{if } Q > 0), \quad -a_n Q(\text{if } Q < 0) \\ V_p &= a_p Q^2(\text{if } Q > 0), \quad +a_n Q^2(\text{if } Q < 0) \end{aligned} \tag{1}$$

The a_p and a_n coefficients and R-square of the $Q - V_p$ relationship for the different PD sources are reported in Table 1. Referring to this table, there is a strong correlation (high R-square) between Q and V_p for corona, free particle in oil and void discharges; however, the correlation is weak (low R-square) for surface discharge in air, surface discharge in oil and discharge in oil.

The $Q - V_p$ relationship is almost symmetric only for source models having free particles in oil or discharge in voids. A PD source in air has a much smaller V_p/Q if compared with a PD source in the oil. Table 1 shows that the type of PD source has a great impact on the relationship between Q and V_p. According to

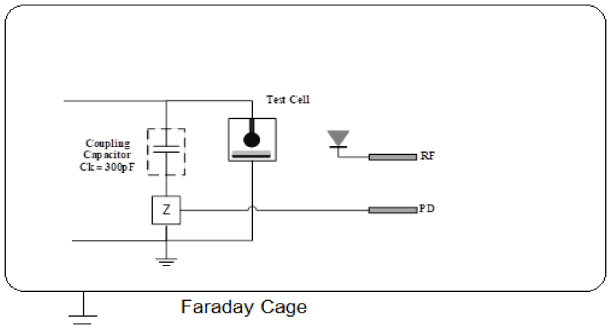

Fig. 1 *Experimental setup (inside the Faraday cage)*

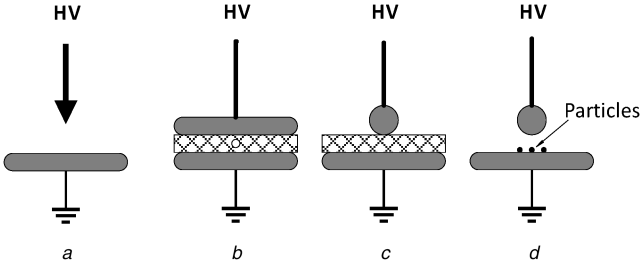

Fig. 2 *Electrode configurations of artificial PD*
(a) Corona and PD in oil, ***(b)*** Void, ***(c)*** Surface discharge in air and oil, ***(d)*** Free particle in oil

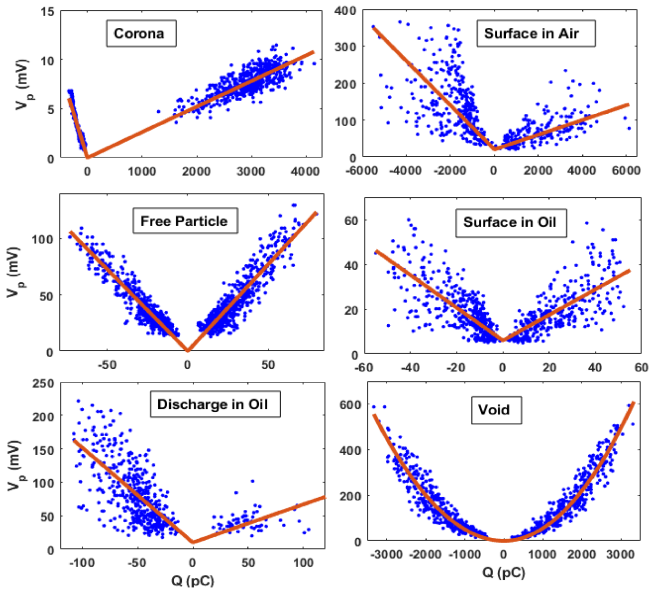

Fig. 3 *$Q - V_p$ relationship for different PD sources*

This is an open access article published by the IET and CEPRI under the Creative Commons Attribution-NonCommercial-NoDerivs License (http://creativecommons.org/licenses/by-nc-nd/3.0/)

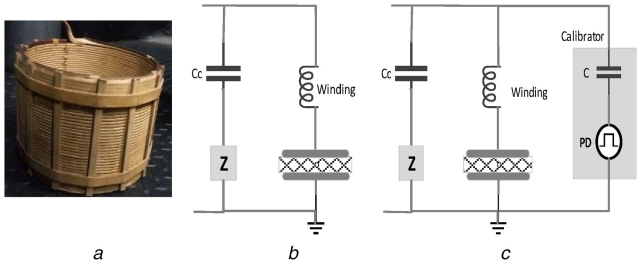

a b c

Fig. 4 *Investigating the impact of the winding on measurements*
(a) Winding, ***(b)*** Experimental setup, ***(c)*** Calibration procedure setup

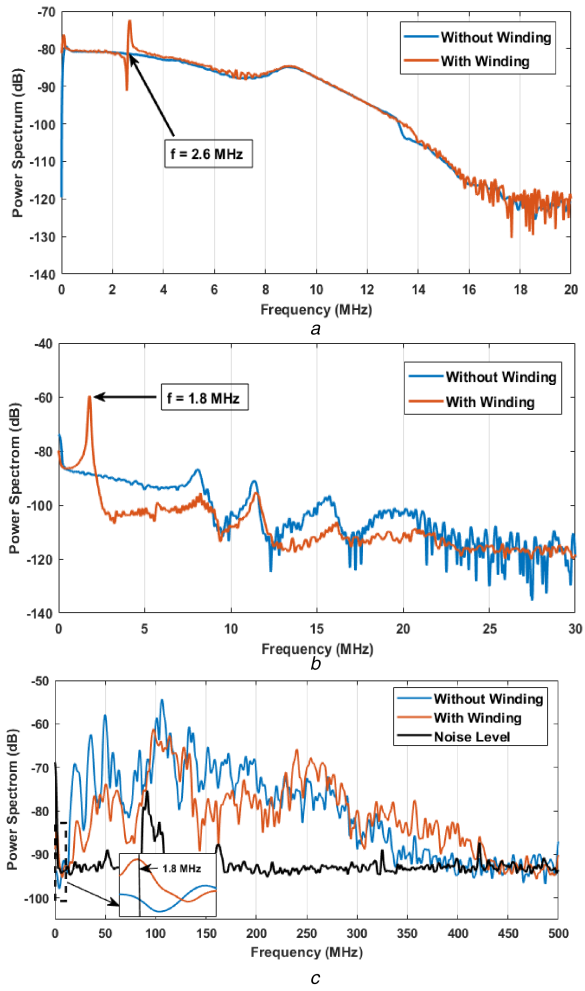

Fig. 5 *Measured current pulse and RF waves power spectrum with and without windings*
(a) Calibrator signal, ***(b)*** PD signal, ***(c)*** RF waves

Reid *et al.* [9], this relationship is highly dependent on the underlying PD pulse shape.

4 PD signal transmitter

The occurrence of PD activity causes an HF current pulse to flow in the windings. On the other hand, when an HF current pulse flows through the wire, EM waves arise into the space. So, the winding will act as a radiating antenna for the RF method and also as a current path for IEC method.

Due to the fact that the current path acts such as a low-pass filter [14] and also because the generated PD current has lower energy at a higher frequency [15, 16], the higher frequencies cannot be detected by the measuring impedance; however, they can be detected by RF probe. Therefore, the transformer winding has an impact on both the measured current and on the RF signals. To study these effects, a coil winding that is shown in Fig. 4*a*, with diameter of 26 cm, height of 15 cm and 35 turns, is connected in series with a void-PD source model as shown in Fig. 4*b*. This setup has been calibrated using a standard PD calibrator with rise time of 35 ns and fall time of 100 ns, as shown in Fig. 4*c*.

Table 1 Correlation between Q and V_p for different PD sources

PD type	a_p	a_n	R-square, %
corona	0.0026	0.018	81
surface in air	0.02	0.06	33
free particle	1.26	1.32	87
surface in oil	0.78	0.98	38
discharge in oil	0.57	1.24	35
void	5.2×10^{-5}	5.6×10^{-5}	85

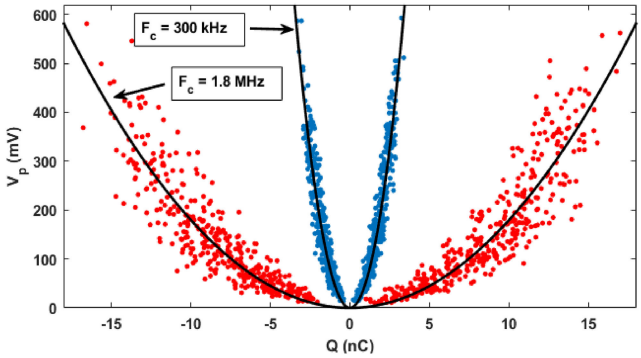

Fig. 6 *$Q - V_p$ relation when the winding is added*

The measured current pulses power spectrum with and without a winding, under calibrator setup and PD source setup are shown in Figs. 5*a* and *b*. It can be seen that adding a winding to the experimental setup results in a new resonant frequency, which is different for the calibrator setup and the PD source setup. These results show that calibration cannot predict the winding effects.

The presence of the winding, thus, changes the characteristics of the radiating antenna and affects the received RF signals. An RF antenna is a form of circuit consisting of an inductance and a capacitance and thus has a resonant frequency. This is the frequency where the capacitive and the inductive reactance cancel each other out. Since the added winding has a low resonance frequency, it behaves effectively such as a capacitance at higher frequencies. On the other hand, if a capacitor is added to the antenna, the resonant frequency will increase, and the antenna will perform better at higher frequencies.

Fig. 5*c* shows the RF waves power spectrum measured by the antenna for a 900 pC internal discharge with and without adding the winding. As shown in this figure, the peak of the RF wave with and without winding adding occurs at 98 and 105 MHz, respectively, and also by adding the winding, the HF characteristic of the waves recorded by the antenna is amplified and the low-frequency recorded waves are attenuated. When the winding is added, the 1.8 MHz RF frequency is also detectable. This is because the resonant frequency of the current pulse occurred at this frequency and it can be detected due to the high amplitude of the current pulse at this frequency.

The winding always has an impact on the RF signals voltage (V_p). However, for Q it depends on the measurement frequency. Fig. 6 shows the relationship between Q and V_p when the winding is added. The electric charge is measured at two frequencies, i.e. 300 kHz and 1.8 MHz, each with a 400 kHz bandwidth. If the charge measurement is performed at a frequency lower than the resonant frequency (300 kHz), the charge is not affected by the winding. However, if this measurement is carried out at a resonant frequency, in this case 1.8 MHz, the calculated charge will be much greater than the actual charge, because the calibration cannot eliminate the winding effect.

The positive (a_p) and negative (a_n) coefficients of the $Q - V_p$ quadratic relationship for the two centre frequencies are reported in Table 2. According to this table, adding the winding causes the RF signal peak voltage to become smaller (by comparing the values of

This is an open access article published by the IET and CEPRI under the Creative Commons Attribution-NonCommercial-NoDerivs License (http://creativecommons.org/licenses/by-nc-nd/3.0/)

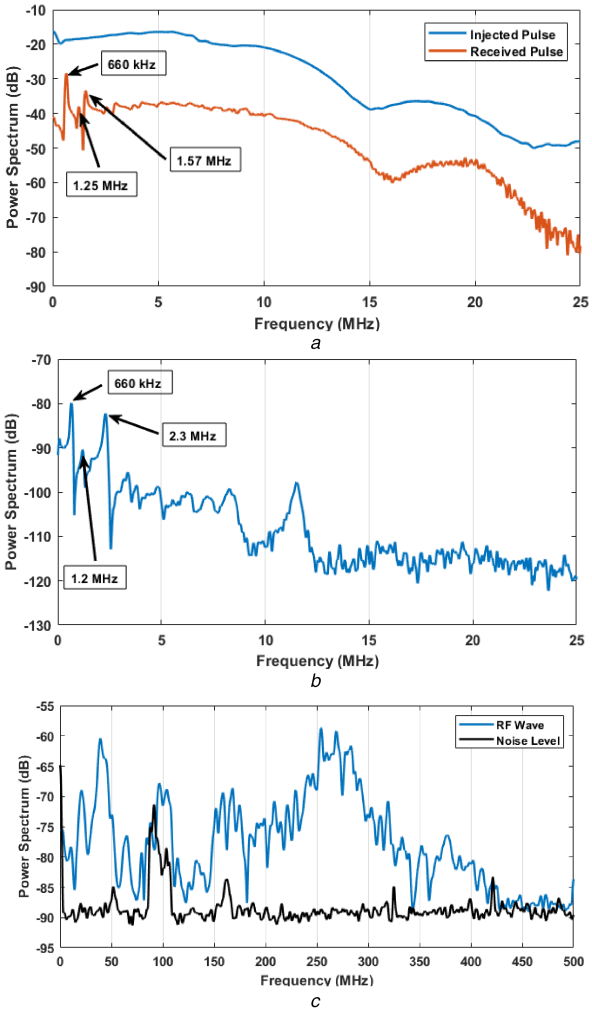

Fig. 7 *Measurement of current pulse and RF wave power spectrum of transformer model*
(a) Calibrator, ***(b)*** PD pulse, ***(c)*** RF wave

a_p and a_n of Table 1 with Table 2). This is because, by adding the winding, the RF emission performs better at a higher frequency, but, on the other hand, the PD pulse energy is higher at a lower frequency.

5 Effect of inner structure

The PD source puts an HF current pulse through the winding and the winding then acts as an antenna and radiates PD current pulse emission. There are many transformer components between the radiated EM waves and the receiver that affect the measured RF signal peaks and apparent charge. Transformer insulation, the transformer tank and the distance between the PD source and receiver antenna are the most important factors that affect the relationship between Q and V_p. These factors are examined in this section.

5.1 Transformer insulation

For transformer oil, the attenuation constant (α) of EM waves is given by [17]

$$\alpha \simeq \frac{\sigma}{2}\sqrt{\frac{\mu}{\varepsilon}} \tag{2}$$

where σ is conductivity, ε is the permittivity and μ is the permeability of oil. According to this equation, when an aged oil is used, where the conductivity $\sigma = 10^{-11}$(s/m) [18] the attenuation is -1.1×10^{-8} dB/m. So, the oil is effectively a lossless path for the propagation of EM waves, and the only difference between the propagations of EM waves in air and oil is that the velocity of waves in the oil is 2/3 the wave velocity in the air because of the higher permittivity.

Table 2 Positive and negative coefficients of $Q - V_p$ quadratic relationship for measurement of Q at different frequencies

Centre frequency	a_p	a_n	*R*-square, %
300 kHz	4.6×10^{-5}	5.1×10^{-5}	83
1.8 MHz	1×10^{-6}	1.1×10^{-6}	78

The other effect of a transformer insulation system is that paper and oil between the winding and the core create two parallel paths for current flow. The transformer's winding and its insulation structure form a complex inductive–capacitive–resistive network that develop a number of resonant frequencies which can be excited by the frequency contents of a PD current pulse [19]. To investigate the effect of these parallel paths, a small transformer model is used to carry out the experiments. The single-phase transformer model is composed of three windings (i.e. primary, secondary and tertiary), the insulating oil and the paper insulation. The cavity defect is placed at the bottom of the winding structure between the primary and secondary windings [20]. This single-phase transformer model is placed in an oil-filled plastic pan and the measurement of RF signal is carried out using a conical antenna placed inside the pan and within 0.5 m distance of the transformer model.

First, measurements are made using a calibrator. The results are shown in Fig. 7*a*. The existence of a capacitance between the winding and the core provides a lower amplitude for the captured pulse in comparison with the injected pulse. The PD pulse attenuation under low frequencies, where the effect of winding is negligible, can be estimated using the calibrator signal. The frequency spectrum of the measured PD pulse is shown in Fig. 7*b*. According to this figure, the calibrator enables accurately identification of the first two resonant frequencies; however, these two pulses have quite different resonant frequencies at higher frequencies. Therefore, if the charge is measured at low frequencies, the insulation effect between the winding and the core can be estimated by application of the PD calibrator, while this measurement under higher frequencies is influenced by the winding structure which cannot be estimated using the calibrator.

In PD pulses, low-frequency waves have a longer wavelength (lower-energy dissipation) so these waves can penetrate longer distances. On the other hand, they will be further attenuated by travelling over longer distances. The HF components have short wavelengths and the energy content is small [15, 16]: the energy of high frequencies gets dissipated faster, so they only penetrate a short distance. As a result of the effect of impedances due to the insulation between the winding and the grounded core, the frequency spectrum of the measured RF wave will be different from that at the source. As shown in Fig. 7*c*, the peak of the RF wave occurs at 255 MHz, while the related frequency for a simple cavity PD source model is 105 MHz as shown in Fig. 5*c*.

By measuring the charge at a lower frequency ($f_c = 300\,\text{kHz}\ and\ \Delta f = 400\,\text{kHz}$), calculated charge is not affected by the insulation. However, the insulation also affects the RF signals and this effect cannot be compensated. Therefore, the insulation affects the $Q - V_p$ relationship. This relationship for void discharge activity in the transformer model is shown in Fig. 8. This data also shows a quadratic relation between data captured using the two methods. The positive and negative coefficients [as defined in Section 3, (1) and Table 1] for this data are 2.1×10^{-5} and 2.2×10^{-5}, respectively, as compared with 5.2×10^{-5} and 5.6×10^{-5} for the earlier test. The value of *R*-square for this data is 70%, as against 85%, which indicates that this relationship is weaker.

5.2 Transformer tank

A transformer tank acts as a cavity resonator for EM waves [21, 22]. The resonant frequencies are given by the following equation for rectangular cavity resonators [23]:

This is an open access article published by the IET and CEPRI under the Creative Commons Attribution-NonCommercial-NoDerivs License (http://creativecommons.org/licenses/by-nc-nd/3.0/)

$$f_{\text{mnp}} = \frac{c_0}{2\sqrt{\varepsilon_r}}\sqrt{\left(\frac{m}{a}\right)^2 + \left(\frac{n}{b}\right)^2 + \left(\frac{p}{c}\right)^2} \quad (3)$$

where f_{mnp} are the cavity resonances, c_0 denotes the speed of light, ε_r is the relative permittivity (is 1 for air and 2.2 for oil) a, b and c are the geometric dimensions of the tank and m, n, p are the mode numbers. As the resonant frequencies increase, the densities of the modes increase accordingly (the higher resonant frequencies are closer together). For this reason, only the first few modes are useful in practise for a closed cavity resonator [23]. So, the number of effective resonant frequencies depends on the size of the transformer tank.

According to Wen [23], radiated RF waves inside the transformer tank can be divided into three frequency bands. Over the low-frequency band (lower than the first resonant frequency), the tank blocks radiating RF waves. In the mid-frequency band (from the first resonant frequency to several times of this frequency), the tank acts as a cavity resonator and amplifies the RF waves. At high frequencies, the tank has no effect.

To investigate the effect of the tank dimensions, a PD test is performed inside both the tanks, i.e. a large tank (Faraday cage) and a small tank (as shown in Fig. 9); with dimensions of 6 m × 6 m × 4 m and 0.4 m × 1 m × 0.5 m, respectively. For the sake of convenience, three bushings are mounted on the tank wall so that the different PD defects can be implemented easily into the transformer model without draining its tank oil. The first five resonant frequency of big and small tanks is given in Table 3.

RF wave output of free metal particles was measured inside the two tanks. The frequency characteristics of RF signals in the small and big transformer tanks are shown in Fig. 10*a*. The first resonant frequencies for a big and small transformer tanks are 35 and 341 MHz, respectively. The results obtained from (3) and the measured results are approximately equal for the first resonance frequency and other resonant frequencies. For the large tank, the resonant frequency band is from 35 MHz (first resonant frequency) to several times of this frequency (around 250 MHz). For the small tank, the number of resonant frequencies increases so that the entire frequency range (341–2000 MHz) is included. As the best frequency bands for measuring EM waves is where a transformer tank acts as cavity resonator, the smaller the size of the tank, the more impact it will have on the measured RF signals.

Fig. 10*b* shows the $Q - V_p$ relationship for the free metal particle inside the small transformer tank. The positive and negative coefficients for this linear relationship are 4.8 and 5.3, respectively. These coefficients are 3.8 and 4 times higher than the coefficients for the big transformer (reported in Table 1). These numbers indicate that the dimensions of the transformer tank have a great influence on the relationship between Q and V_p and also that negative PDs of free metal particles have relatively higher energy than the positive PDs with the same charge at higher frequencies.

5.3 Distance

Another factor that affects the measured RF signals is the distance between the PD source and the signal receiver (antenna) [24]. To investigate the effect of distance, simultaneous measurements of Q and V_p were performed for free metal particle and void-PD sources at different distances between source and receiver.

Fig. 11 shows the relationship between $Q - V_p$ for the free metal particle source and the void-PD source at four different distances. For both sources, with the increase of the distance between PD and the antenna, the measured peak of the RF signal decreases. For the free metal particle source, the relationship between Q and V_p is linear at different distances; however, for a void-PD source this relationship changes from quadratic to linear with increasing distance.

The positive and negative coefficients of the $Q - V_p$ relationship for the free metal particle source at different distances are given in Table 4. From both Fig. 11*a* and Table 4, the positive and negative coefficients of the relationship decrease as the distance increases.

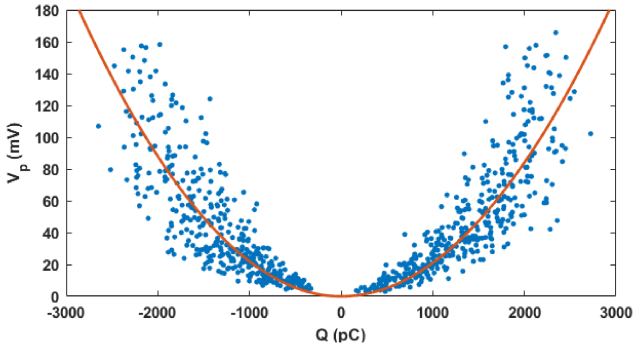

Fig. 8 *Relationship between Q and V_p for void discharge in small size transformer model*

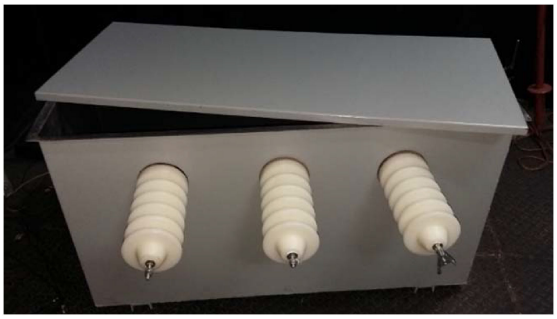

Fig. 9 *Small transformer tank with three bushings*

Table 3 Big and small tanks first five resonant frequencies

Big tank		Small tank	
mnp	f_{mnp}, MHz	mnp	f_{mnp}, MHz
110	35	011	335
111	50	110	405
302	105	101	476
024	157	131	650
107	262	022	675

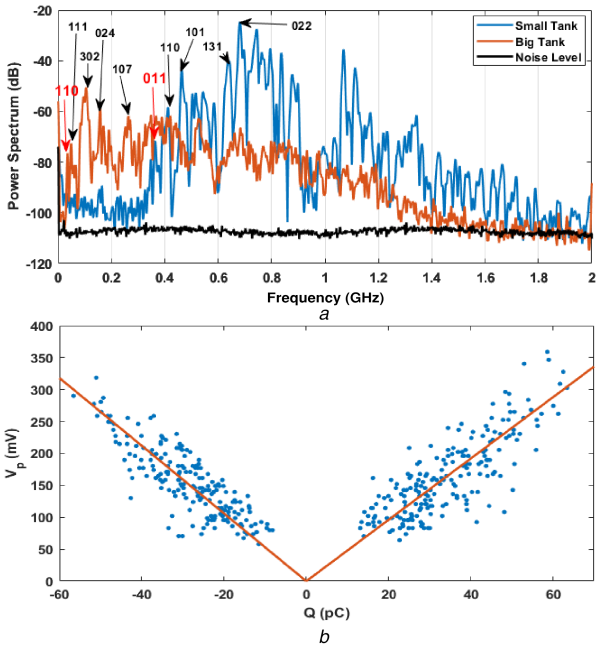

Fig. 10 *Effect of transformer tank size in*
(a) Frequency characteristic of RF waves, ***(b)*** $Q - V_p$ relationship of free particle inside small tank

This is an open access article published by the IET and CEPRI under the Creative Commons Attribution-NonCommercial-NoDerivs License (http://creativecommons.org/licenses/by-nc-nd/3.0/)

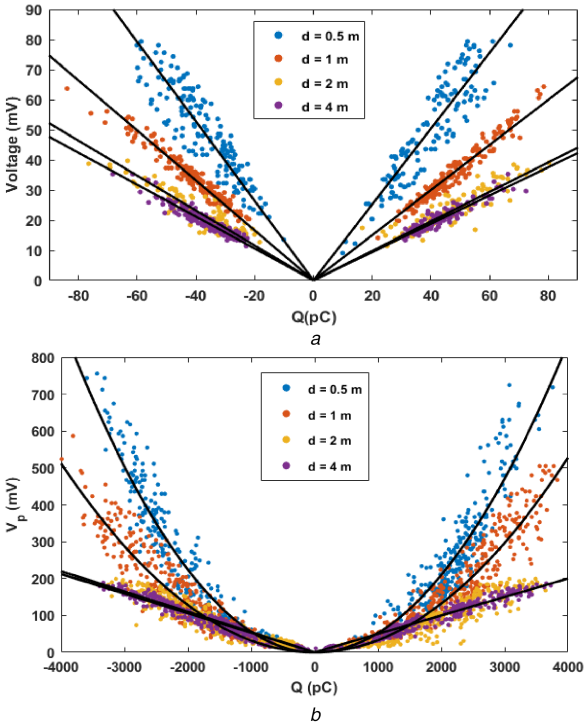

Fig. 11 *Effect of distance in $Q - V_p$ relationship*
(a) For a free metal particle PD source, ***(b)*** For a void-PD source

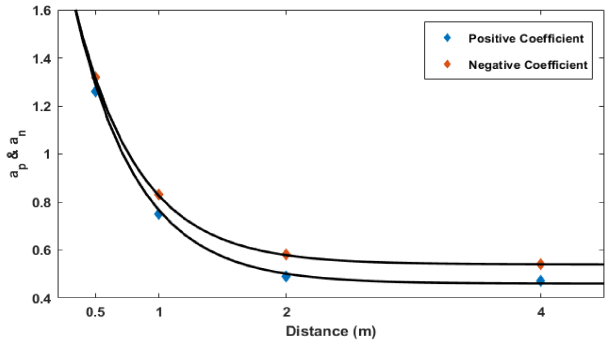

Fig. 12 *Positive and negative coefficients relation with distance*

The following exponential function can be used for establishing a relationship between the positive and negative coefficients with distance variation d:

$$a_p = 2.25e^{-2d} + 0.46$$
$$a_n = 2.1e^{-2d} + 0.54 \quad (4)$$

Fig. 12 shows graphically the positive and negative coefficient relationships with the distance. According to (4), the relation between the coefficients and distance is composed of two parts: one part is constant and the other part is exponentially related to the distance. So the signals received by the antenna consist of two parts, one that is independent of the distance, and the other that decreases exponentially as the distance increases.

For the void source, with increasing distance, not only is the amplitude of the received RF waves decreasing, but also the form of the $Q - V_p$ relationship also changes. To determine how this relationship changes with distance, the following formula is fitted to the void-PD data at different distances:

$$V_p = a_p Q^r \text{ (if } Q > 0), \quad + a_n Q^s \text{ (if } Q < 0) \quad (5)$$

The coefficients of this equation for different distances are given in Table 5 below. As is clear from this table, the $Q - V_p$ relationship changes from a parabolic-type equation to a linear-type equation as distance increases. The relationship for the positive and negative

Table 4 Positive and negative coefficients of $Q - V_p$ relationship for free metal particle source at different distances

Coefficient	Distance, m			
	$d = 0.5$	$d = 1$	$d = 2$	$d = 4$
a_p	1.26	0.75	0.49	0.47
a_n	1.32	0.83	0.58	0.54

Table 5 Positive and negative coefficients of $Q - V_p$ relationship for void source at different distances [as in (5)]

Coefficient	Distance, m			
	$d = 0.5$	$d = 1$	$d = 2$	$d = 4$
a_p	6.6×10^{-6}	8×10^{-5}	0.005	0.036
a_n	8.5×10^{-6}	8×10^{-5}	0.009	0.023
r	2.26	1.89	1.3	1.04
s	2.24	1.89	1.23	1.1

charges are almost the same ($r \simeq s$); however, the positive (a_p) and negative (a_n) coefficients in (5) are different.

The S transform (ST) has been used to investigate the cause of a change in the type of $Q - V_p$ relationship. ST is a time–frequency representation technique [25], which can be described as

$$A(\tau, f) = \left| \int_{-\infty}^{+\infty} x_n(t) \frac{|f|}{\sqrt{2\pi}} e^{(((t-\tau)^2 f^2)/2)} e^{-j2\pi f t} dt \right| \quad (6)$$

where $x_n(t)$ is the RF wave and τ represents the location over the timeline. Fig. 13 shows an ST time–frequency representation of the normalised void RF pulse at two different distances. The colour in Fig. 13 indicates the value of A in (6). According to this figure, the recorded RF waves can be classified under two frequency bands: the mid-frequency band and the HF band. The mid-frequency band signal does not change with distance; however, the HF band signal decreases if the distance increases. So, the HF band of RF signal is not detectable at a 4 m distance. On the other hand, by increasing the distance, the $Q - V_p$ relationship changes from a non-linear to a linear relationship. Therefore, the non-linear relationship between Q and V_p, for void-PD source, is due to the non-linear relationship between HF EM waves and Q.

The results show that the $Q - V_p$ relationship depends on the distance between the PD source and the antenna, which is due to the presence of HF EM waves. So, by measuring the RF signals in the mid-frequency band (the frequency range in which the transformer tank acts as a cavity resonator), this relationship is linear and independent of the distance for both the floating metal particle and void-PD sources. V_p is measured using a low-pass filter with a cut-off frequency of 200 MHz. The results of this measurement are shown in Fig. 14. As it is clear from Fig. 14, the relationship between Q and V_p is linear for floating metal particle and almost linear ($r = s = 1.15$) for void discharge and independent of distance between PD source and antenna for both PD sources.

6 Summary and conclusion

A detailed study on the parameters that impact on the $Q - V_p$ relationship for standard IEC60270 type PD monitoring (Q) and RF monitoring with an antenna (V_p) of the same PD activity is presented in this paper. This has been done using laboratory measurements on simple PD source models, a simple small transformer model and two different sizes of transformer tank.

The effect of PD source is investigated for six PD models using simultaneous acquisition of the RF and IEC60270 signals for each PD pulse. This has been achieved by plotting the RF signal peaks against the corresponding measured apparent charge on a 2D scatter plot. It was observed that this relationship is dependent on the type of source. The RF/IEC ratio is greater for PD sources in

This is an open access article published by the IET and CEPRI under the Creative Commons Attribution-NonCommercial-NoDerivs License (http://creativecommons.org/licenses/by-nc-nd/3.0/)

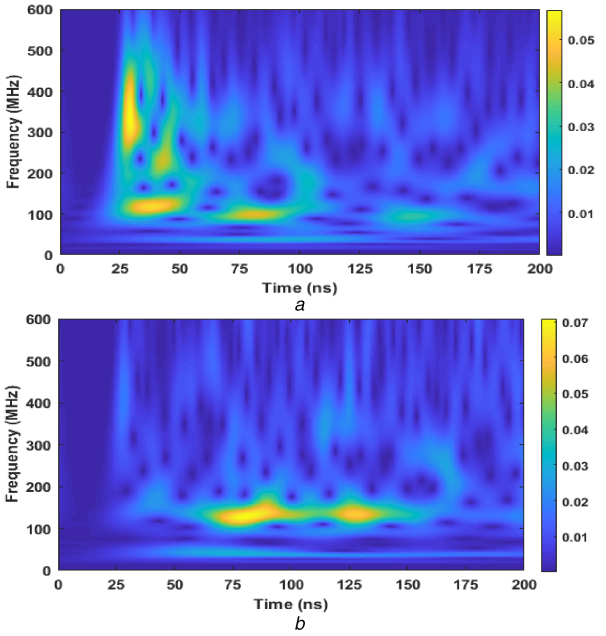

Fig. 13 *ST representation of RF signal for distance between void-PD source and antenna is*
(a) 0.5 m, ***(b)*** 4 m

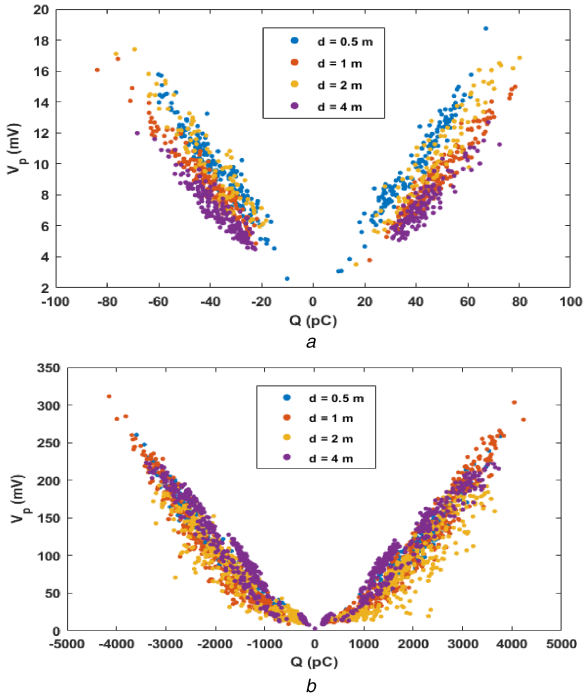

Fig. 14 *$Q - V_p$ relation for measurement of V_p using 200 MHz low-pass filter for*
(a) Floating metal particle, ***(b)*** Void

oil than in air. For discharge in oil and surface discharge in oil correlation between the two methods is weak (i.e. the coefficients much smaller than 1.0). However, for free metal particles and PD void model, the correlation between these two methods is strong (i.e. the coefficients close to 1).

The effect of the presence of a transformer winding on both measurement methods outcome is determined by adding a winding to the void-PD source. The presence of this winding results in the development of new resonant frequencies in the current signal, which cannot be predicted by application of a calibrator and the only way to eliminate this effect is to measure electric charge at frequencies lower than the resonant frequency. The winding also changes the frequency characteristic of the RF signals, which causes a relative change in $Q - V_p$ relationship.

The impact of inner structure is examined by taking into account the effect of the insulating system, transformer tank and the distance between PD source and RF probe. The effect of the insulating system on IEC method is high; however, this effect can be compensated using the calibrator measurement. The insulating system also affects RF method measurement results, which cannot be compensated for. A transformer tank operates as cavity resonator within a certain range of frequencies for EM waves. As shown in previous sections, smaller transformer tank sizes result in an increase in the magnitude of captured RF signals.

The effect of the distance between a PD source and the antenna is investigated by simultaneous measurements of Q and V_p at different distances for floating metal particles and the void-PD sources. It is shown that the $Q - V_p$ relationship is linear and independent of the distance for both floating metal particles and void-PD sources when the measured PD signals are captured over a frequency range in which the transformer tank acts as a cavity resonator.

These results provide a method for calibration of an RF PD measurement setup in order to take into account the effects of some of the variables (such as distance between PD source and RF probe) which cause differences between the two methods' measurement results. To achieve the ultimate goal, in the future, methods should be developed to compensate for such complex system effects.

7 References

[1] Rusov, V., Zhivodernikov, S.: 'Transformer condition monitoring'. Int. Conf. Condition Monitoring and Diagnosis 2008 CMD 2008, 2008, pp. 1012–1014

[2] Chakravorti, S., Dey, D., Chatterjee, B.: '*Recent trends in the condition monitoring of transformers*', (Springer-Verlag, London, UK, 2013), p. 277

[3] Firuzi, K., Vakilian, M., Darabad, V.P., *et al.*: 'A novel method for differentiating and clustering multiple partial discharge sources using S transform and bag of words feature', *IEEE Trans. Dielectr. Electr. Insul.*, 2017, **24**, (6), pp. 3694–3702

[4] Firuzi, K., Vakilian, M.: 'Partial discharges pattern recognition of power transformer defect model by LBP & HOG features'

[5] Firuzi, K., Vakilian, M.: 'A novel online partial discharge monitoring method through stream clustering of signals'

[6] Tenbohlen, S., Denissov, D., Hoek, S.M., *et al.*: 'Partial discharge measurement in the ultra-high-frequency (UHF) range', *IEEE Trans. Dielectr. Electr. Insul.*, 2008, **15**, (6), pp. 1544–1552

[7] Cleary, G.P., Judd, M.D.: 'UHF and current pulse measurements of partial discharge activity in mineral oil', *IEE Proc. Sci. Meas. Technol.*, 2006, **153**, (2), pp. 47–54

[8] Judd, M.D., Yang, L., Hunter, I.B.B.: 'Partial discharge monitoring for power transformers using UHF sensors part 1: sensors and signal interpretation', *IEEE Electr. Insul. Mag.*, 2005, **21**, (2), pp. 5–14

[9] Reid, A.J., Judd, M.D., Fouracre, R.A., *et al.*: 'Simultaneous measurement of partial discharges using IEC60270 and radio-frequency techniques', *IEEE Trans. Dielectr. Electr. Insul.*, 2011, **18**, (2), pp. 444–455

[10] Yoshida, M., Kojima, H., Hayakawa, N., *et al.*: 'Evaluation of UHF method for partial discharge measurement by simultaneous observation of UHF signal and current pulse waveforms', *IEEE Trans. Dielectr. Electr. Insul.*, 2011, **18**, (2), pp. 425–431

[11] Jahangir, H., Akbari, A., Werle, P., *et al.*: 'Possibility of PD calibration on power transformers using UHF probes', *IEEE Trans. Dielectr. Electr. Insul.*, 2017, **24**, (5), pp. 2968–2976

[12] Constantine, A.B.: 'Antenna theory: analysis and design', in Birtcher, C.R., Yang, B. (Eds.): '*Microstrip antennas*' (John Wiley & Sons, 2005, 3rd edn.), p. 1065

[13] Lopez-Roldan, J., Tang, T., Gaskin, M.: 'Optimisation of a sensor for onsite detection of partial discharges in power transformers by the UHF method', *IEEE Trans. Dielectr. Electr. Insul.*, 2008, **15**, (6), pp. 1634–1639

[14] Wang, Z., Li, J., Sofian, D.M.: 'Interpretation of transformer FRA responses – part I: influence of winding structure', *IEEE Trans. Power Deliv.*, 2009, **24**, (2), pp. 703–710

[15] Lemke, E.: 'Guide for partial discharge measurements in compliance to IEC60270'. *CIGRE Technical Brochure*, 2008, vol. **366**

[16] Hauschild, W., Lemke, E.: '*High-voltage test and measuring techniques*' (Springer, 2014)

[17] CIGRE Working Group A2.18: 'Guide for life management techniques for power transformers'.*CIGRÉ Brochure 227*, 2003

[18] Wentworth, S.M.: '*Applied electromagnetics: early transmission lines approach*' (John Wiley & Sons, 2007)

[19] Agoris, P.D.: 'Sensitivity verification of radio frequency partial discharge detection in high voltage equipment', TU Delft, Delft University of Technology, 2009

[20] Rostaminia, R., Saniei, M., Vakilian, M., *et al.*: 'Accurate power transformer PD pattern recognition via its model', *IET Sci. Meas. Technol.*, 2016, **10**, (7), pp. 745–753

[21] Tenbohlen, S., Hoek, S.M., Denissov, D., *et al.*: 'Electromagnetic (UHF) PD diagnosis of GIS, cable accessories and oil–paper insulated power

This is an open access article published by the IET and CEPRI under the Creative Commons Attribution-NonCommercial-NoDerivs License (http://creativecommons.org/licenses/by-nc-nd/3.0/)

transformers for improved PD detection and localization'. CIGRE Session 2006, 2006
[22] Markalous, S.M., Tenbohlen, S., Feser, K.: 'Detection and location of partial discharges in power transformers using acoustic and electromagnetic signals', *IEEE Trans. Dielectr. Electr. Insul.*, 2008, **15**, (6), pp. 1576–1583
[23] Wen, G.: '*Foundations for radio frequency engineering*' (World Scientific, 2015)
[24] Coenen, S., Tenbohlen, S., Markalous, S.M., *et al.*: 'Sensitivity of UHF PD measurements in power transformers', *IEEE Trans. Dielectr. Electr. Insul.*, 2008, **15**, (6), pp. 1553–1558
[25] Stockwell, R.G., Mansinha, L., Lowe, R.P.: 'Localization of the complex spectrum: the S transform', *IEEE Trans. Signal Process.*, 1996, **44**, (4), pp. 998–1001

This is an open access article published by the IET and CEPRI under the Creative Commons Attribution-NonCommercial-NoDerivs License (http://creativecommons.org/licenses/by-nc-nd/3.0/)